

Heat Uptake and the Thermohaline Circulation in the Community Climate System Model, Version 2

PETER R. GENT AND GOKHAN DANABASOGLU

National Center for Atmospheric Research, Boulder, Colorado*

(Manuscript received 16 February 2004, in final form 27 April 2004)

ABSTRACT

Ocean heat uptake and the thermohaline circulation are analyzed in present-day control, 1% increasing CO₂, and doubled CO₂ runs of the Community Climate System Model, version 2 (CCSM2). It is concluded that the observed 40-yr trend in the global heat content to 300 m, found by Levitus et al., is somewhat larger than the natural variability in the CCSM2 control run. The observed 40-yr trend in the global heat content down to a depth of 3 km is much closer to trends found in the control run and is not so clearly separated from the natural model variability. It is estimated that, in a 0.7% increasing CO₂ scenario that approximates the effect of increasing greenhouse gases between 1958 and 1998, the CCSM2 40-yr trend in the global heat content to 300 m is about the same as the observed value. This gives support for the CCSM2 climate sensitivity, which is 2.2°C.

Both the maximum of the meridional overturning streamfunction and the vertical flow across 1-km depth between 60° and 65°N decrease monotonically during the 1% CO₂ run. However, the reductions are quite modest, being 3 and 2 Sv, respectively, when CO₂ has quadrupled. The reason for this is that the surface potential density in the northern North Atlantic decreases steadily throughout the 1% CO₂ run. In the latter part of the doubled CO₂ run, the meridional overturning streamfunction recovers in strength back toward its value in the control run, but the deep-water formation rate across 1-km depth between 60° and 65°N remains at 85% of the control run value. The maximum northward heat transport at 22°N is governed by the maximum of the overturning, but the transport poleward of 62°N appears to be independent of the deep-water formation rate.

1. Introduction

When projections of the future climate are made using coupled general circulation models, the two aspects of the ocean circulation that are most frequently analyzed are the ocean heat uptake and the North Atlantic thermohaline circulation (see, e.g., Houghton et al. 2001). The interest in ocean heat uptake was increased by the observational study of Levitus et al. (2000). Using observations between the mid-1950s and mid-1990s, they documented large decadal variability and an increasing trend in heat content over the 40-yr period. This raises the question: can this increasing trend be explained as natural variability, or is it a signal of the anthropogenic forcing changes that the earth has experienced over the last 50 yr? This question has been addressed before using different climate models. Levitus et al. (2001), Reichert et al. (2002), Barnett et al. (2001), and Sun and Hansen (2003) all conclude that the trend is not natural variability but is a signal of the changed an-

thropogenic forcing. The first two of the climate models used had flux adjustments, the third has subsequently been improved upon (see Gent et al. 2002), and the last has a “non-negligible climate drift” in its control run. We ask the same question in this paper, using the updated Community Climate System Model, version 2 (CCSM2), which is documented in Kiehl and Gent (2004). Our conclusion, that there is only a small probability that the observed increase in heat content down to 300 m is due to natural variability, was also found in all these earlier studies.

Virtually every future climate scenario performed using climate models has been analyzed to show the possible evolution of the North Atlantic thermohaline circulation. The majority of these scenarios show a modest reduction of the maximum of the meridional overturning streamfunction over the period 2000–2100 or as CO₂ doubles from the present-day value (see Houghton et al. 2001). The reason for this is a warming and freshening of the surface ocean in the northern North Atlantic, which leads to a more stable vertical density profile. Many of the models included in the Intergovernmental Panel on Climate Change (IPCC) report use flux adjustments. However, the same result of a modest reduction for the same reason is found in the third Hadley Centre Coupled Ocean–Atmosphere General Circula-

* The National Center for Atmospheric Research is sponsored by the National Science Foundation.

Corresponding author address: Dr. Peter R. Gent, National Center for Atmospheric Research, Boulder, CO 80307-3000.
E-mail: gent@ucar.edu

tion Model (HadCM3), which has no flux adjustments (see Thorpe et al. 2001). A few models show a more dramatic decline in the thermohaline circulation over the next century, and some show no reduction in the strength of the thermohaline circulation. The first version of the Climate System Model (CSM1) was in this latter category. Gent (2001) shows that the surface warming was balanced by higher surface salinity, with almost no change in surface density in the northern North Atlantic. Kiehl and Gent (2004) document large improvements in the North Atlantic and Arctic Oceans in the CCSM2 compared to the CSM1, and the response of the North Atlantic thermohaline circulation has changed between the two model versions. In the CCSM2, there is a modest reduction in the strength of the North Atlantic thermohaline circulation in the run where CO_2 increases by $1\% \text{ yr}^{-1}$.

The ocean component of the CCSM2 and the three experiments run are described in section 2. Section 3 contains analysis of the heat content variability and trends, and changes in the North Atlantic thermohaline circulation are shown in section 4. Section 5 contains conclusions and a discussion of the CCSM2 results compared to observed trends.

2. The model and experiments

The ocean component uses the Parallel Ocean Program (POP) code, which was developed at the Los Alamos National Laboratory (see Smith et al. 1992). The model solves the primitive equations in general orthogonal coordinates in the horizontal with the hydrostatic and Boussinesq approximations. The grid uses spherical coordinates in the Southern Hemisphere, but in the Northern Hemisphere the pole is displaced into Greenland at 80°N , 40°W . The horizontal grid has 320 (zonal) \times 384 (meridional) grid points, and the resolution is uniform in the zonal direction but not in the meridional direction. In the Southern Hemisphere, the meridional resolution is 0.27° at the equator, gradually increasing to 0.54° at 33°S , and is constant at higher latitudes. There are 40 levels in the vertical, whose thickness monotonically increases from 10 m near the surface to 250 m in the deep ocean. The minimum depth is 30 m, and the maximum depth is 5.5 km. An implicit free surface formulation is used for the barotropic equations (see Dukowicz and Smith 1994). The surface freshwater flux is converted into an implied salt flux using a constant reference salinity. Therefore, although the sea surface height varies locally, the ocean volume remains fixed. The domain is global, which includes Hudson Bay, the Mediterranean Sea, and the Persian Gulf. The time step used is 1 h, which is small enough that no Fourier filtering is required around the displaced Greenland pole.

The horizontal viscosity is a Laplacian operator that is anisotropic following the formulation of Smith and McWilliams (2003) and uses different coefficients in the

east–west and north–south directions. Both coefficients are spatially and temporally variable and depend on the local rates of shear and strain based on the scheme of Smagorinsky (1963), and the minimum background horizontal viscosity is $1000 \text{ m}^2 \text{ s}^{-1}$. The vertical mixing scheme is the K -profile parameterization scheme of Large et al. (1994). In the ocean interior, the background diffusivity varies in the vertical from $0.1 \times 10^{-4} \text{ m}^2 \text{ s}^{-1}$ near the surface to $1.0 \times 10^{-4} \text{ m}^2 \text{ s}^{-1}$ in the deep ocean. The background viscosity has the same vertical profile but is larger by a factor of 10. The parameterization of the effects of mesoscale eddies is that of Gent and McWilliams (1990), which mixes along isopycnals with a Laplacian operator and uses an additional eddy-induced advection of potential temperature and salinity. This parameterization, with a constant coefficient of $600 \text{ m}^2 \text{ s}^{-1}$, is implemented using the skew flux form of Griffies (1998). The ocean component also uses a new equation of state for seawater (see McDougall et al. 2003). Only a summary of the ocean component physics and parameters is given here, and further details can be found in Smith and Gent (2002).

This paper analyzes results from three experiments using the CCSM2 climate model. The first is a control (CON) experiment that is intended to simulate the “present day” climate of 1990. All the greenhouse gases in the atmosphere were set to the 1990 levels; for example, the carbon dioxide level was set to 355 ppm. The ocean was initialized using January mean climatological fields from Levitus et al. (1998) and Steele et al. (2001) in the Arctic Ocean. The other three components were initialized using fields from stand-alone runs. Kiehl and Gent (2004) document this experiment in more detail, including some small changes that were made at year 350. These changes have no impact on the results presented in this work.

The second experiment is a standard experiment of increasing CO_2 levels in the atmosphere by $1\% \text{ yr}^{-1}$, labeled the CO_2 run. This experiment started at the end of year 220 of the control run, after most of the adjustment of the solution has occurred (see Kiehl and Gent 2004). This experiment was integrated for 150 yr until year 370. The CO_2 doubled after 70 yr at year 290 and quadrupled after 140 yr at year 360. The third experiment branches from the CO_2 run at the end of year 290, with the CO_2 level kept constant thereafter at twice the level in the CON run. This is labeled the 2CO_2 run and has been integrated for 130 yr up to year 420. Unfortunately, more than 1.5 yr after these experiments were completed, an error was found in March 2004. In the atmosphere component, CO_2 was expressed as both a volume mixing ratio and a mass mixing ratio. In the CO_2 and 2CO_2 experiments, the volume mixing ratio was increased by $1\% \text{ yr}^{-1}$ and kept at its doubled value. However, the mass mixing ratio was not and remained at its initial value corresponding to 355 ppm. Initial estimates suggest that this error underestimates the effect of increasing CO_2 by just under 10%. We decided not to change the results

presented in sections 3 and 4, but the error does slightly affect the comparison of the results with the Levitus et al. (2000) observations in section 5. However, it does not change any of the conclusions from this work that are also presented in section 5.

3. Heat content changes

We will follow Levitus et al. (2000) and consider heat content changes over two depth ranges: from the surface down to 300 m and from the surface down to 3 km. We will show results in terms of the average potential temperature for each volume considered for two reasons. The first is that this normalizes the heat content changes with respect to the varying sizes of the different ocean basins, and the second is that the results are then in terms of familiar temperature units. The average potential temperature can be converted into heat content by multiplying by $\rho_0 c_p$ times the volume of ocean in the various domains. In the model, $\rho_0 c_p$ is constant and equal to $4.1 \times 10^6 \text{ J } ^\circ\text{C}^{-1} \text{ m}^{-3}$. Results will be shown from six different domains: the Southern, Pacific, Indian, Atlantic, Arctic, and Global Oceans. The Southern Ocean is defined to be all of the ocean south of 33°S . Note that these are all large to very large ocean basins, except for the Arctic Ocean. This has been included not only because it will be informative to compare results from a small basin but also because the CCSM2 has realistic Arctic Ocean variability in its sea ice and ocean components (see Holland 2003). This is in stark contrast to CSM1, which had very poor Arctic variability (see the discussion in Kiehl and Gent 2004). Finally, Kiehl and Gent (2004) show that the CCSM2 takes about 150 yr for most variables to come into an equilibrium state, so that we choose to show heat content changes between years 200 and 1000. This period includes all of the CO₂ and 2CO₂ runs.

Most of the adjustment in the upper-ocean heat content has taken place by year 200, so that there are very small trends in the average temperature of the upper 300 m over years 200–1000. However, this is not the case in the deep ocean, which is continuously losing heat over this period. The annual average temperatures over the six ocean basins down to 3 km are shown in Fig. 1. There are small, but significant, downward trends in all oceans except the Arctic Ocean. The temperature of the Global Ocean decreases almost linearly from 4.72°C at year 200 to 4.28°C at year 1000, which is a 0.44°C decrease over 800 yr. This is equivalent to a uniform heat loss over the entire ocean of 0.19 W m^{-2} . The Levitus et al. (1998) value, which was used for the ocean initial condition, is 4.64°C , so that the global ocean down to 3 km loses just under 8% of its heat content over 1000 yr. There are comparable losses in the other major ocean basins, but the Arctic Ocean behaves very differently. The average temperature rises from 1.24°C at year 200 to 1.75°C at year 1000. However, there is considerable multidecadal variability, so that the tem-

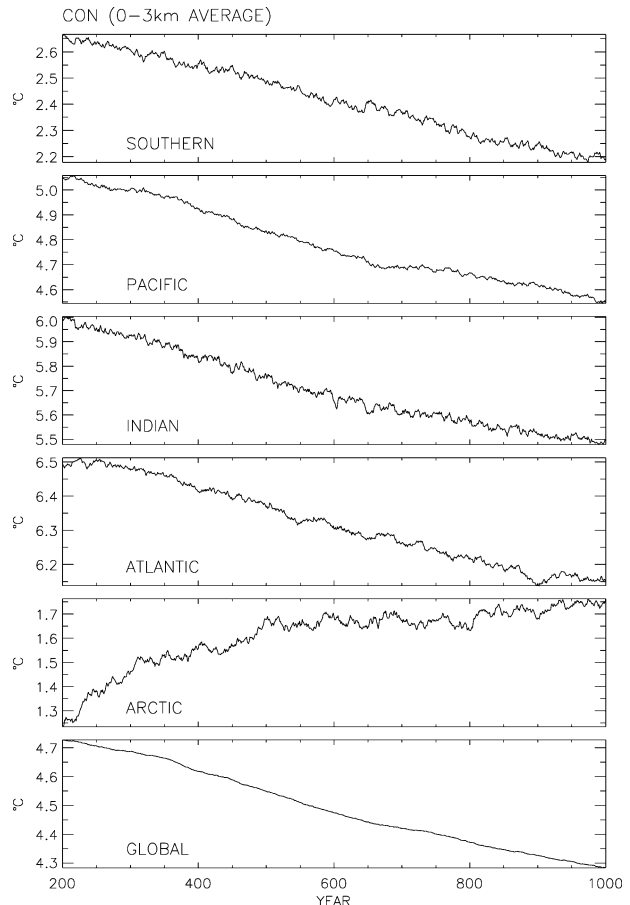


FIG. 1. Annual and 0–3-km-average potential temperature from the CON run.

perature rise is not uniform over the 800 yr. This compares to the much more uniform temperature decrease in the other ocean basins, which are all much larger than the Arctic Ocean.

Figure 2 shows the average temperatures down to 3 km of the six basins in the CO₂ run. The figure shows heat uptake in all ocean basins at a rate that increases uniformly in time during the run. The Global Ocean value increases from 4.72°C at year 220 to 5.22°C at year 370. The initial 40-yr trend in the CO₂ run is a 0.04°C increase, and the overall 150-yr trend is a 0.5°C increase over the run. These trends are 2 and 6 times, respectively, that in the CON run and of the opposite sign. The other large ocean basins behave similarly, with positive trends that are much larger than the negative trends in the CON run. The Arctic Ocean average temperature increases from 1.25°C at year 220 to 2.45°C at year 370. This is a 150-yr trend of 1.2°C , which is again considerably larger than the 0.5°C 800-yr trend of the CON run, but in this case the trends are both positive. The trends in ocean heat content over the upper 300 m and 3 km of the CON run are much smaller than the trends in the CO₂ run. This means that, for the Global

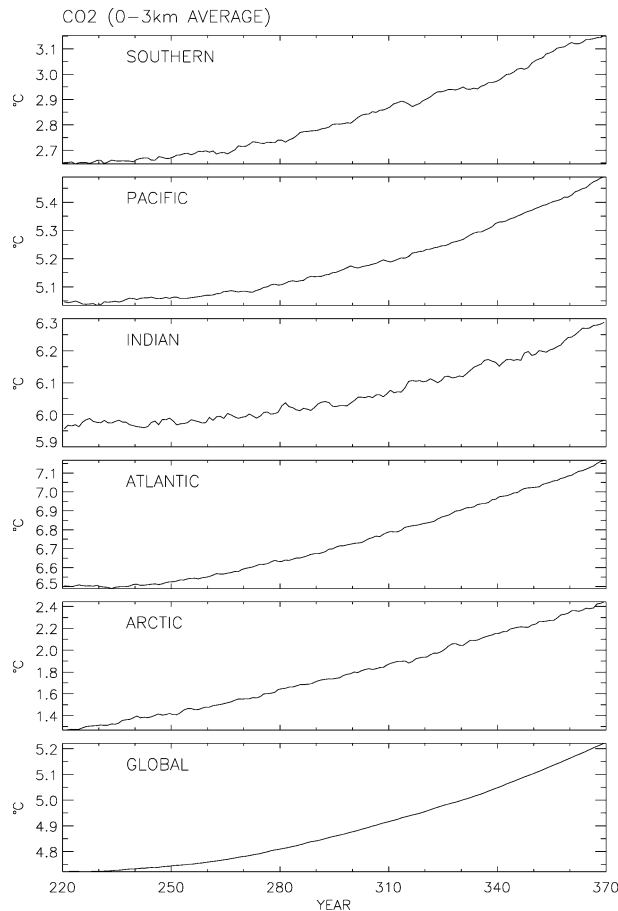


FIG. 2. Same as in Fig. 1, but from the CO₂ run.

Ocean and large ocean basins, using the CO₂ or (CO₂ - CON) time series does not make much difference to the trend values. Therefore, the trends will only be shown from the CON and CO₂ runs, rather than from the (CO₂ - CON) time series. Usually, the latter is shown because the trends in the control run are larger.

Levitus et al. (2000) show observational results on ocean heat content changes between the mid-1950s and the mid-1990s. Thus, we decided to analyze the CCSM2 runs in terms of 40-yr trends, which are again plotted as changes in the volume-averaged potential temperature. The values are plotted at the center of the 40-yr period, so the values for the CON run are plotted between years 220 and 980. Figure 3 shows the 40-yr trends over the upper 300 m from the CON run for the six different ocean domains. There are two important points to note from Fig. 3. First, for the individual ocean basins there is about the same number of positive and negative 40-yr trends, which confirms that there are small overall trends in these quantities in the last 800 yr of the CON run. The Global Ocean does show a small decrease in heat content with more negative than positive values. Second, the amplitude of the 40-yr

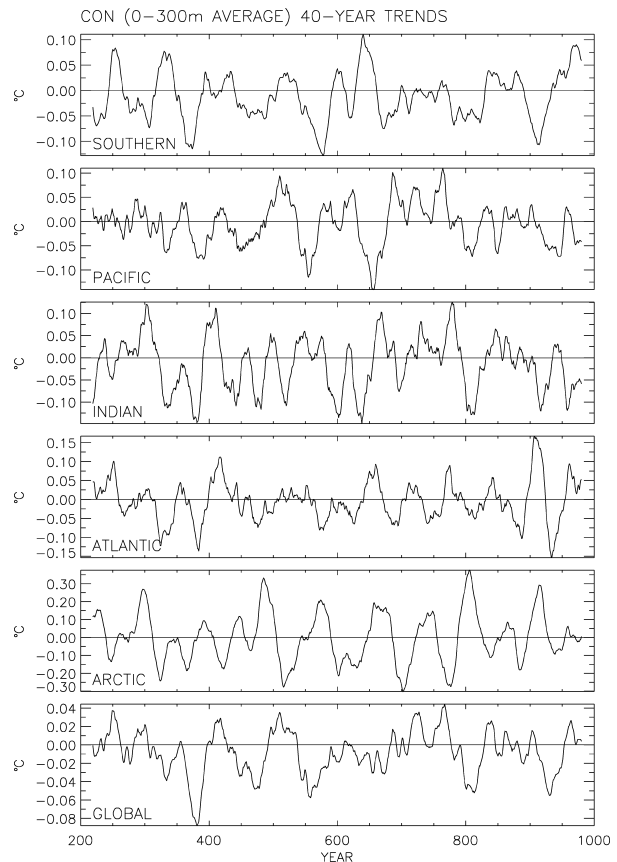


FIG. 3. The 40-yr trends for the 0–300-m-average potential temperature from the CON run.

trends increase as the size of the basin decreases. In the Arctic Ocean, the 40-yr trends reach $\pm 0.3^\circ\text{C}$; in the other ocean basins, the 40-yr trends are between $\pm 0.15^\circ\text{C}$; and the Global Ocean 40-yr trends are more on the order of $\pm 0.05^\circ\text{C}$. Figure 4 shows the 40-yr trends from the upper 300 m from the CO₂ run plotted between years 240 and 350. The first point to make is that all the trends are significantly positive; the smallest 40-yr trend is 0.2°C at the start of the Southern Ocean time series. Again, the largest trends are in the smallest basin, with the Arctic Ocean 40-yr trend starting at 0.38°C and increasing to $>0.8^\circ\text{C}$ at the end of the run. Note that for the Arctic, the minimum 40-yr trend in the CO₂ run of 0.38°C is just larger than the maximum 40-yr trend in the CON run of 0.36°C .

In the larger basins, the initial 40-yr trends in the CO₂ run are larger by about a factor of 2 than the maximum trends in the CON run. In most basins, the CO₂ run trends increase later in the run, but an interesting exception is the Indian Ocean, where the trends are not monotonically increasing. The initial 40-yr trend in the Global Ocean is 0.27°C , which is at least 4 times as large as the maximum positive 40-yr trend from the time series of the CON run shown in Fig. 3. Because

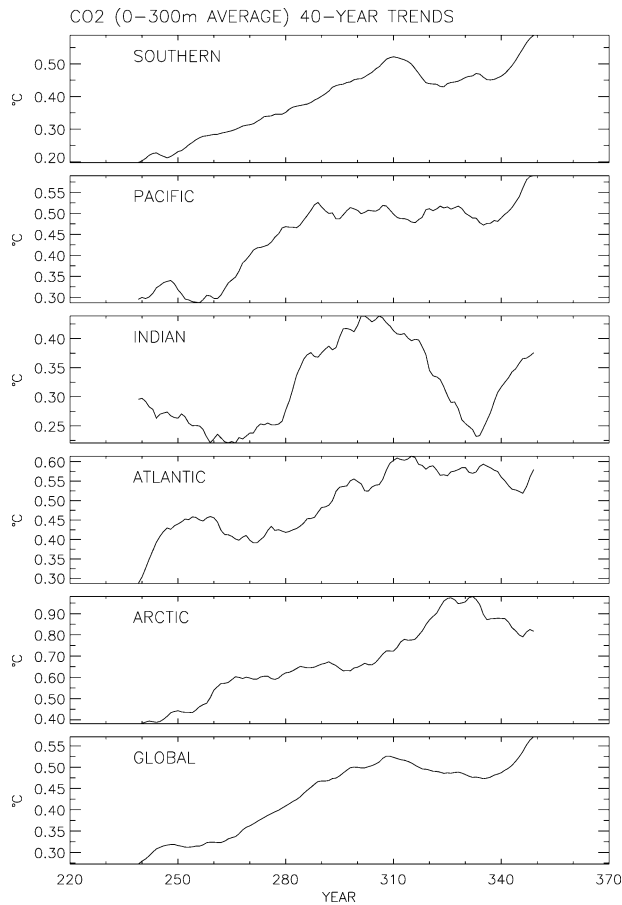


FIG. 4. Same as in Fig. 3, but from the CO₂ run.

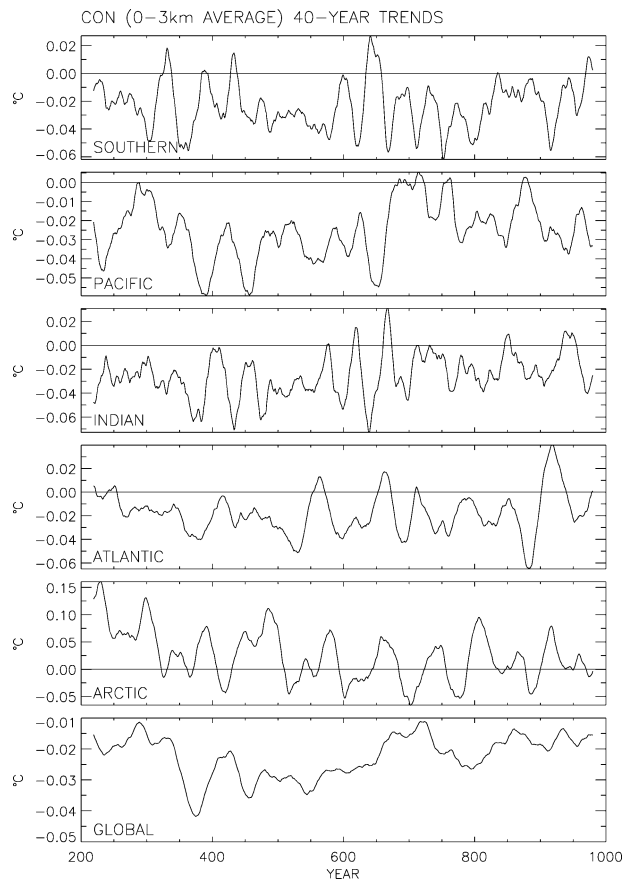


FIG. 5. The 40-yr trends for the 0–3-km-average potential temperature from the CON run.

the initial 40-yr trends in the large basins and Global Ocean from the CO₂ run are larger by factors of 3 or more, it is essentially certain that they cannot arise from the natural variability in the CON run. Whether upper-ocean heat content changes can be used to diagnose climate change will be discussed much more thoroughly in section 5.

The 40-yr trends in the CON and CO₂ runs for average temperature changes down to 3 km are shown in Figs. 5 and 6. The downward trend in the CON run heat content shows up clearly in Fig. 5, with all the large basins showing mostly negative values. The Global Ocean has all negative values. The Arctic Ocean is warming slightly and again has by far the largest natural variability, with 40-yr trends of $\pm 0.1^\circ\text{C}$ being regularly seen. The maximum range of 40-yr trends in the large basins is 0.1°C in the Indian and Atlantic Oceans. The maximum range in the Global Ocean values is 0.04°C . In the CO₂ run, Fig. 6 shows that the 40-yr trends are essentially increasing monotonically in time. However, the initial 40-yr trends are quite small, being 0.05°C in the Southern and Atlantic Oceans, 0.03°C in the Pacific Ocean, and 0.01°C in the Indian Ocean. Comparison with Fig. 5 shows that the initial 40-yr trends in the

Indian and Pacific Oceans are well within the natural variability of the CON run. The initial CO₂ run trends in the Atlantic, Southern, and Global Oceans are only just larger than the natural variability trends. Thus, the initial 40-yr trends in the heat content down to 3 km in the CO₂ run are not clearly separated from the natural model variability. These 40-yr trends increase significantly later in the CO₂ run, but it is not until about year 300 that the 40-yr trends are large enough to be virtually certain that they are not natural variability. The clear inference from these results is that, early in the CO₂ run, heat content changes down to 300 m are much more likely to be out of the range of natural variability than the heat content changes down to 3 km.

4. North Atlantic thermohaline circulation

The most frequently used measure of the strength of the thermohaline circulation is the maximum value of the meridional overturning streamfunction in the North Atlantic. The time series of this measure over the 1000-yr CON run is shown in Fig. 7a. At the start of the run, the maximum values are about 20 Sverdrups ($1 \text{ Sv} \equiv 10^6 \text{ m}^3 \text{ s}^{-1}$) but start to decrease after about 50 yr. The

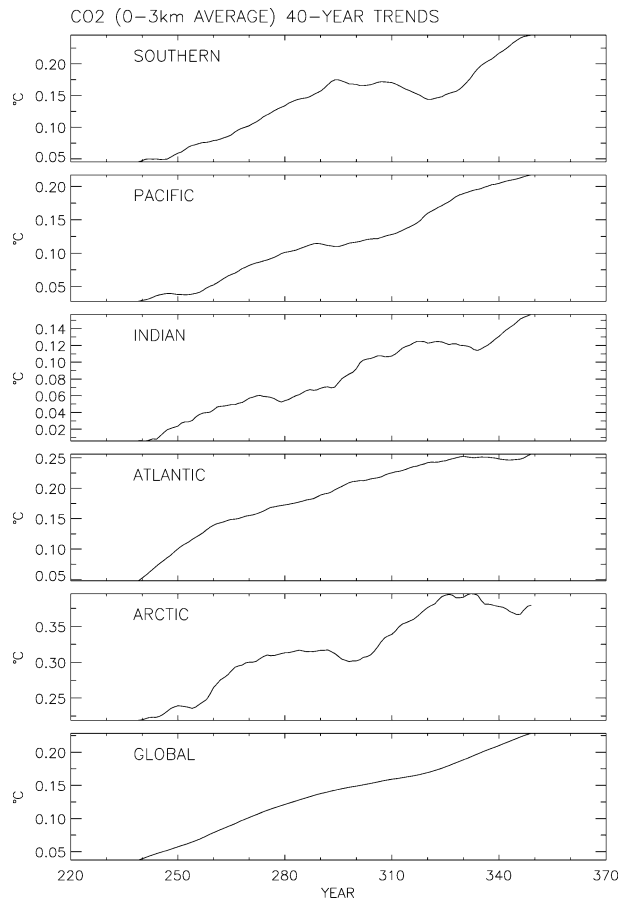


FIG. 6. Same as in Fig. 5, but from the CO₂ run.

overturning has equilibrated after about 170 yr, which is consistent with the model drifts becoming very small after 150 yr. The average value of the maximum overturning over the 200–1000-yr period is 15.7 Sv. This is much smaller than in the CSM1 version, where it was about 30 Sv (see Bryan 1998), and is much closer to the best observational estimates, which average about 17 Sv (see Hall and Bryden 1982; Roemmich and Wunsch 1985).

Figure 7b shows the average meridional overturning streamfunction from years 201–220 of the CON run. This streamfunction is calculated from the Eulerian mean velocity, but the eddy-induced velocity has always been diagnosed from numerical models to be very small throughout the Atlantic Ocean north of 33°S (see, e.g., Danabasoglu et al. 1994). The maximum overturning occurs at about 35°N at a depth of 850 m. The zero contour, which separates the North Atlantic Deep Water from the Antarctic Bottom Water, occurs at a depth of between 2.5 km near the equator to 3 km at about 60°N. This is about 1 km too shallow compared to initializing the model with Levitus et al. (1998) data but is an extremely common feature of noneddy-resolving ocean climate components that use z coordinates. Gent (2001)

suggests that a different measure of the strength of the thermohaline circulation is the amount of deep water formed by dense water spilling over the Denmark Strait and the Iceland–Scotland ridge. He proposed a measure of this deep-water formation to be the vertical transport across the 1-km-depth surface between 60° and 65°N. An important reason to use 1-km depth, and not a shallower depth, is that 1 km intersects the zero line of the overturning streamfunction (see Fig. 7b). Thus, this measure captures all of the deep water formed by southward flow through the Denmark Strait and over the Iceland–Scotland ridge. One reason to use the Gent (2001) measure is that it is easier to estimate from observations than the maximum of the overturning streamfunction. Figure 7b shows that the vertical transport between 60° and 65°N across the 1-km-depth surface is about 8 Sv, which is about half of the maximum overturning.

Figure 8a shows the time series of the North Atlantic maximum overturning between years 200 and 420 from the CON, CO₂, and 2CO₂ runs. Note that the amplitude of the natural variability is about 3 Sv in all three runs. For the first 40 yr of the CO₂ run, the time series overlays that of the CON run but then gradually starts to decrease. The two lines do not really separate until after the CO₂ value has doubled at year 290. The overturning continues to weaken, and the average value between years 350 and 370, which bracket the time when CO₂ has quadrupled, is 12.9 Sv. Thus, in the CO₂ run, the maximum overturning has decreased by about 1 Sv at the time of doubling and 3 Sv when CO₂ has quadrupled. The time series in the 2CO₂ run is interesting in that the maximum overturning continues to decrease for the first 70 yr, when its average value is 13.6 Sv, but then begins to recover its strength. After another 50 yr, at year 410, the average value is 14.3 Sv, and it continues to increase back toward the CON run average of 15.8 Sv.

Figure 8b shows the time series of the Gent (2001) measure of the thermohaline circulation strength—namely the vertical transport across the 1-km-depth surface between 60° and 65°N from the CON, CO₂, and 2CO₂ runs between years 200 and 420. The average value in the CON run is 8.3 Sv, with the natural variability being about ± 1 Sv. In the CO₂ run, the curves again cannot be separated over the first 40 yr, and then deep-water formation steadily decreases. The average value at year 290 when CO₂ has doubled is 7.3 Sv, and the average around year 360 is 6.2 Sv when CO₂ has quadrupled. This behavior is very similar to that of the maximum overturning, but the overall percentage decrease of 25% is larger in this measure. The time series from the 2CO₂ run is again interesting. The deep-water formation continues to decrease over the first 70 yr to a value just under 7 Sv, and then it appears to equilibrate to a value of 7 ± 1 Sv. Thus, in the CCSM2, the North Atlantic deep-water formation rate with doubled CO₂ is reduced from the CON run by about 1.3 Sv.

Therefore, the maximum overturning and the deep-

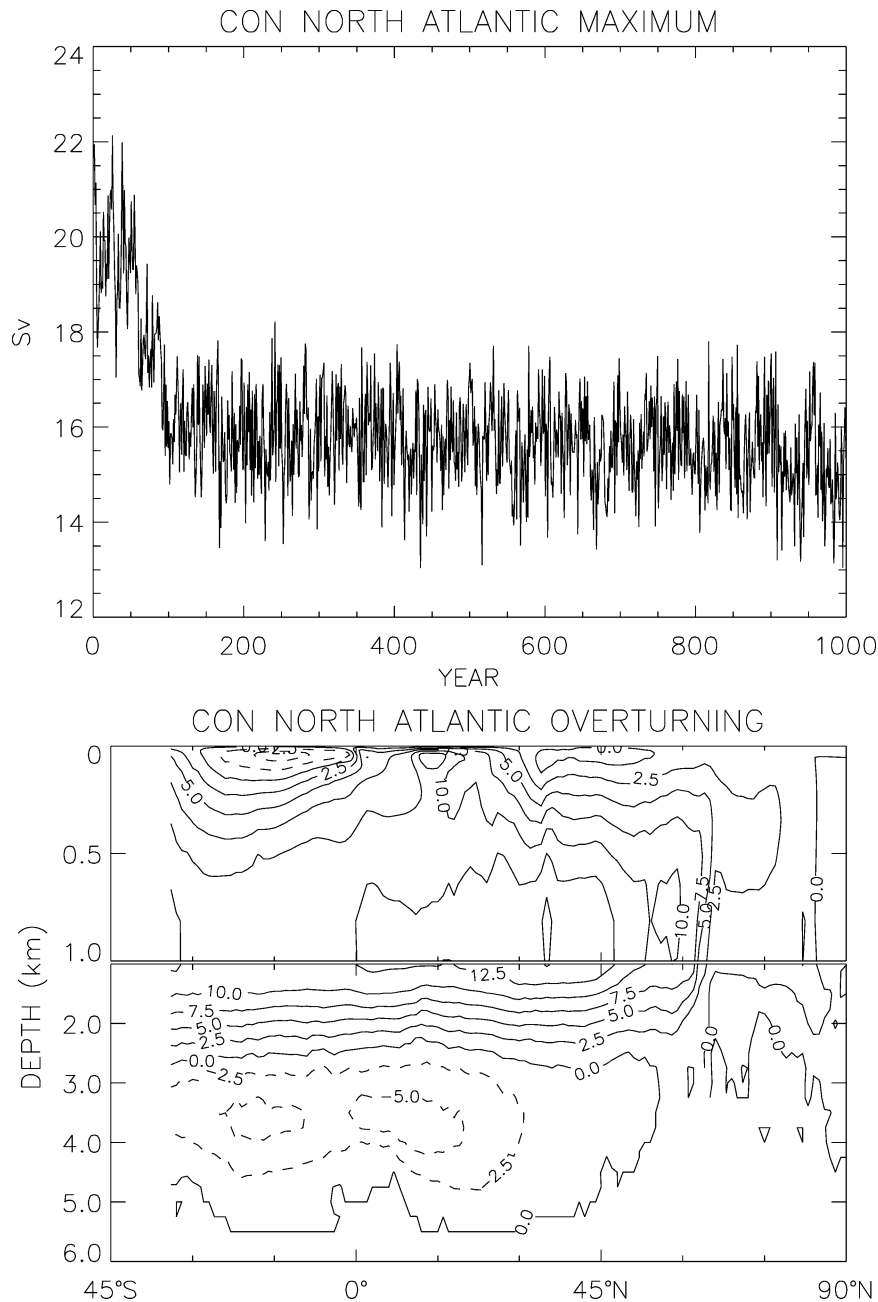


FIG. 7. (a) Time series of the maximum meridional overturning streamfunction from the North Atlantic and (b) the average overturning streamfunction between years 201–220 from the CON run; units are Sv.

water formation rate in the North Atlantic differ over the last part of the doubled CO_2 run. The maximum overturning continues to recover toward the value in the CON run, while the deep-water formation equilibrates at a rate of about 85% of that of the CON run. This illustrates the fact that the maximum overturning should not be the only measure of the strength of the thermohaline circulation. It should also be characterized by

the measure of deep-water formation over the Denmark Strait and Iceland–Scotland ridge, in addition to the maximum overturning.

The strength of the overturning has implications for the northward heat transport by the ocean in the North Atlantic. This transport is shown in Fig. 9 from four 20-yr averages from the three runs. The times shown are years 201–220 of the CON run, 350–369 of the CO_2

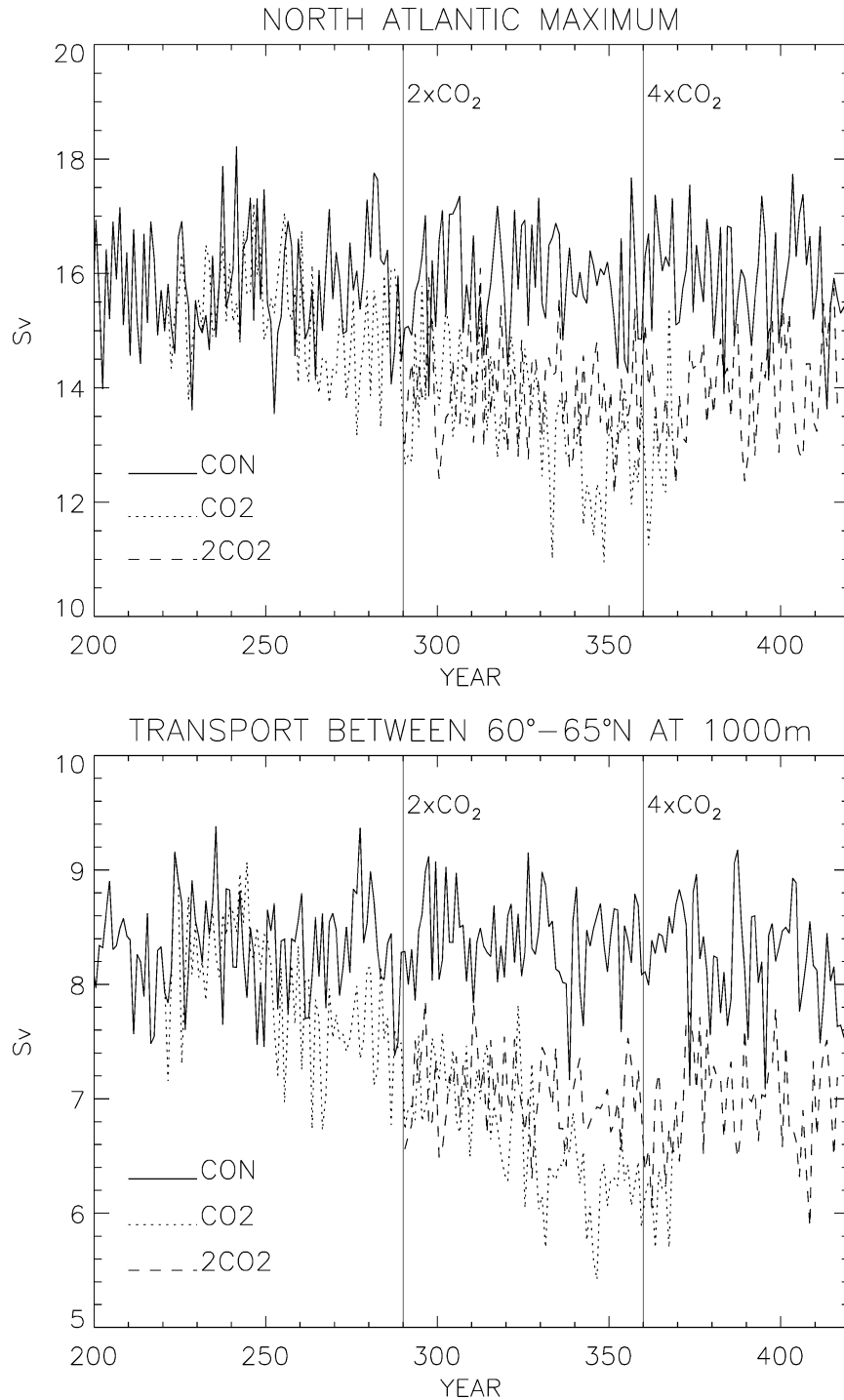


FIG. 8. Time series of (a) the maximum of the meridional overturning streamfunction and (b) the transport across 1-km depth between 60° and 65° N in the North Atlantic from the CON, CO₂, and 2CO₂ runs. Doubling and quadrupling times are shown by the vertical lines.

run, and 350–369 and 397–416 of the 2CO₂ run. In the CON run, the northward heat transport is 0.4 petawatts (pW) across 0° and a maximum of 0.83 pW at 22° N. These are both somewhat smaller than the best estimates

from observations (see Fig. 6 in Trenberth and Caron 2001). The smallest heat transport occurs at the end of the CO₂ run when CO₂ has quadrupled. The maximum of 0.75 pW at that time is about 10% less than in the

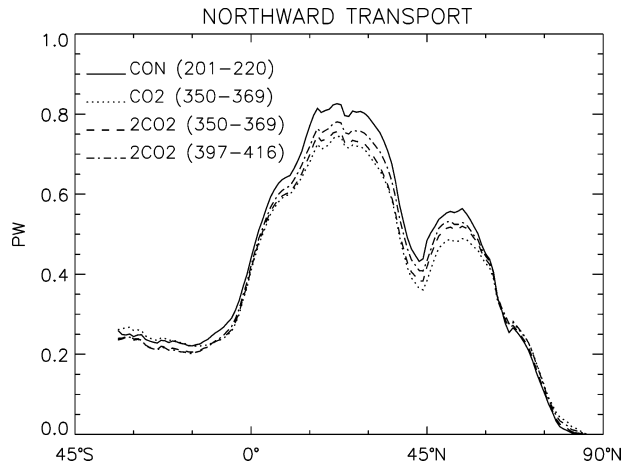


FIG. 9. Northward heat transport in the North Atlantic averaged from years 201–220 from the CON run, 350–369 from the CO₂ run, and 350–369 and 397–416 from the 2CO₂ run; units are petawatts.

CON run. In the 2CO₂ run, the northward heat transport is recovering back toward the CON run values, with the transport being larger at the end of the run compared to 50 yr earlier. The heat transport poleward of 62°N does not change significantly in all three runs. These results are consistent with the demonstration that the maximum northward heat transport in the North Atlantic is directly proportional to the maximum of the meridional overturning streamfunction. This was first demonstrated by Böning et al. (1996) and has been found to hold in many model studies since (see, e.g., Wood et al. 1999). Thus, the maximum northward heat transport, which occurs at about 22°N, is set by the maximum overturning, which occurs at about 35°N. In contrast, the northward heat transport poleward of 62°N appears to be almost independent of the rate of deep-water formation at high latitudes.

The reasons for the modest reduction in the North Atlantic thermohaline circulation are relatively straightforward to diagnose. In the deep-water formation regions in the northern North Atlantic between 50° and 70°N, including the Labrador Sea, the average surface potential density reduces almost linearly throughout the CO₂ run and is about 0.7 kg m⁻³ lighter when CO₂ has quadrupled. In all the runs, there is a fairly linear relation between changes in surface density, average boundary layer depth, and the overturning strength. A consequence of the lighter surface water is a reduction in the average boundary layer depth in the region, so that deep-water formation does not reach so deep. The lighter surface potential density is due to both a 2.7°C increase in SST and a 0.5-psu decrease in surface salinity at the end of the CO₂ run. The temperature increase is caused by positive heat flux into the region, but there is a modest reduction in the total freshwater flux over the region. Further analysis of the CO₂ run showed that the reduced salinity is mostly caused by the advection of fresher

waters from the Arctic Ocean via the boundary currents along the northeast and east coasts of Greenland. Compared to the start of the CO₂ run, these currents are substantially stronger and the transported water has a much-reduced salinity at the quadrupling time of CO₂.

In the 2CO₂ run, the surface water continues to get less dense for the first 70 yr of the run. However, this trend then disappears, and it remains fairly constant thereafter. This is again reflected in the ocean boundary layer depth and in the strength of the deep-water formation diagnostic of flow across the 1-km depth between 60° and 65°N shown in Fig. 8b. It is not clear why the maximum meridional overturning continues to strengthen late in the 2CO₂ run. This could be due to changes in the wind forcing or the heat and freshwater fluxes to the ocean component. For example, Saenko et al. (2003) have recently shown that the North Atlantic overturning is sensitive to the atmospheric meridional moisture transport in the southern midlatitudes.

5. Discussion and conclusions

Figures 3–6 show 40-yr trends in the heat content down to 300 m and 3 km from the CCSM2 control and 1% yr⁻¹ increasing CO₂ runs. We now compare these model results with the observational study of Levitus et al. (2000), who looked at heat content changes between the mid-1950s and mid-1990s. However, an error in this analysis has recently been found (S. Levitus 2004, personal communication). This mostly affects the heat content values from the 1990s, and the revised estimates of the trends from the 1950s to the 1990s are likely to be two-thirds of the values reported in Levitus et al. (2000).

Levitus et al. (2000) show decadal variations with a maximum amplitude of ±0.2°C in the Indian Ocean, ±0.15°C in the Atlantic and Pacific Oceans, and ±0.1°C in the Global Ocean for changes down to 300 m. Decadal variations of this size are often found in the CCSM2 CON run, except in the Global Ocean where the maximum amplitude is ±0.07°C. For changes down to 3 km, Levitus et al. (2000) show decadal variations of about ±0.03°C in the Atlantic, Indian, and Pacific Oceans and of ±0.01°C in the Global Ocean. Again, decadal variations of this size are often found in the CON run, except in the Global Ocean, where they are ±0.006°C. Thus, the amplitude of decadal variability in the CCSM2 is comparable to that diagnosed by Levitus et al. (2000). It is often assumed that the amplitude of natural variability in coarse resolution climate models is considerably smaller than reality, but this is not the case with ocean heat content variability in the CCSM2. In fact, the variability might have been a little higher, if variations in solar input or volcanic activity had been included in the CON run. The revised Levitus et al. (2000) estimate of the 40-yr trend in global ocean heat content is likely 0.2°C down to 300 m and 0.04°C down to 3 km. Figures 3 and 5 show that the Global Ocean 40-yr trends in the CON run are ±0.06°C down to

300 m and $\pm 0.02^\circ\text{C}$ down to 3 km. If we assume that the model variability is a little low, the conclusion is that the observed 40-yr increase down to 300 m is very likely not due to natural variability. However, the observed 40-yr increase down to 3 km is considerably closer to values in the CON run, so that there is some chance that this is due to natural variability.

We now try to compare the observed increase in ocean heat content with the results of the 1% CO_2 increasing run. The observed level of CO_2 at Mauna Loa, Hawaii, has increased from 315 ppm in 1958 to 368 ppm in 1998. If this is interpreted as a constant percentage increase over 40 yr, then the percentage is 0.4%. The effects of increases in other greenhouse gases during this period are also significant, and it is estimated that the earth has been experiencing radiative changes approximately equivalent to a $0.7\% \text{ yr}^{-1}$ increasing CO_2 experiment over the period 1955–95 (see Houghton et al. 2001). We proceeded using the assumption that the heat content 40-yr trends in the CO_2 run should be multiplied by 0.7 for comparison with the revised Levitus et al. (2000) results. The error in the CO_2 run described at the end of section 2 means that this factor should be increased by up to 10%. However, we decided not to change this factor because there is considerable uncertainty in this $0.7\% \text{ yr}^{-1}$ estimate.

Figure 10 shows two histograms of the 40-yr trends in the global heat content from the CON and CO_2 run values multiplied by 0.7. Note that the CON run values have been multiplied by the ratio of the number of data points in the CO_2 run (110) to the number of data points in the CON run (760). Figure 10a shows the comparison for the heat content down to 300 m. The clear separation between the 40-yr trends in the CON and $0.7 \times \text{CO}_2$ runs is obvious, even for the smaller 40-yr trends near the beginning of the CO_2 run. Figure 10b shows the comparison for the heat content down to 3 km. Now the separation between the CON run and the smaller 40-yr trends near the beginning of the CO_2 run is much smaller. The separation would be even smaller if the overall heat loss trend shown in Fig. 1 was eliminated so that the CON values in Fig. 10b were centered around zero. The revised Levitus et al. (2000) 40-yr trends from observations are likely to be about 0.2° and 0.04°C , respectively. Both these values occur near the beginning of the $0.7 \times \text{CO}_2$ run (see Fig. 10). Despite the error in the CO_2 run and the uncertainties in the comparison described above, these results show that the rate of ocean heat uptake in the CCSM2 is about right to reproduce the revised observed 40-yr trends. This result would be best confirmed in an experiment to reproduce the climate of the twentieth century, but such a run has not been performed using the CCSM2.

We believe that three conclusions can be drawn from this heat uptake study. The first is that heat content changes down to 300 m are much more useful than those down to 3 km to diagnose climate trends and distinguish them from natural variability. We note that heat content

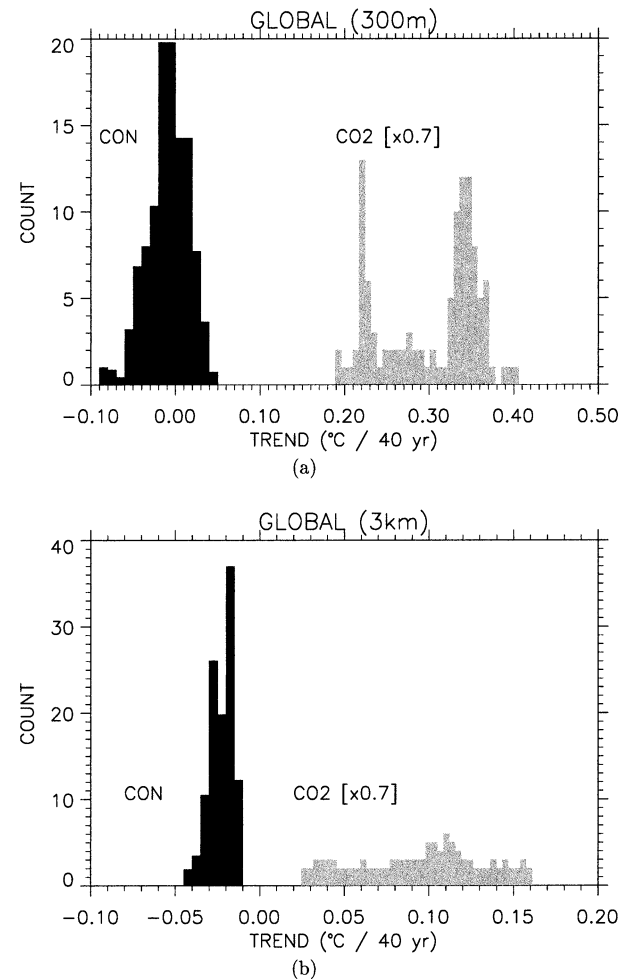


FIG. 10. Histogram of the 40-yr trends in the global ocean heat content from the CON run, and the CO_2 run multiplied by 0.7: (a) down to 300 m with a bin size of 0.01°C and (b) down to 3 km with a bin size of 0.005°C .

changes down to 300 m are likely to be quite well documented from observations compared to changes down to 3 km because of the far greater number of shallow observations. Second, the Levitus et al. (2000) revised 40-yr trend of about 0.2°C down to 300 m very likely cannot be explained as natural variability because it is much too large. This conclusion agrees with the results of Levitus et al. (2001), Barnett et al. (2001), Reichert et al. (2002), and Sun and Hansen (2003). This appears to be a very robust result across quite a wide range of climate models. Note that this conclusion could not be made if the observations had only shown a 20-yr trend of 0.1°C , instead of the larger 40-yr trend. Thus, the trends in ocean heat content need to be over as long a time as possible, and it is very useful that observed trends can be reliably made over 40 yr. If the revised observed 40-yr trend of 0.2°C down to 300 m is assumed to be correct, then a third conclusion is that the rate of ocean heat uptake in the CCSM2 is about right. This

gives support for CCSM2's climate sensitivity of 2.2°C, which is one of the smaller values from the climate models used in the Houghton et al. (2001) report.

In the 1% CO₂ run, both the maximum of the North Atlantic meridional overturning streamfunction and the flow across 1-km depth between 60° and 65°N diminish. At the time when CO₂ is quadrupled, the reductions are 3 and 2 Sv, respectively. The main reason for these reductions is that the surface water is continuously getting less dense during the run, and the depth of convection is reduced. In the doubled CO₂ run, the overturning decreases slowly for about 70 yr but then starts to recover and return to the value in the control run. In contrast, the flow across 1-km depth between 60° and 65°N slowly decreases for about 70 yr but then varies around a value 85% of the control run. Our fourth conclusion is that both the maximum of the overturning streamfunction and the flow across 1-km depth between 60° and 65°N should be used to diagnose the North Atlantic thermohaline circulation. These two measures behave differently in the doubled CO₂ run. As mentioned earlier, the maximum of the overturning streamfunction is extremely difficult to estimate from observations. One problem is that it has a sizable annual cycle and interannual variability. In contrast, the Gent (2001) measure of vertical flow across the 1-km-depth surface between 60° and 65°N is steadier and more easily estimated from ocean observations, although this is not at all straightforward. The modest reduction in the thermohaline circulation in the 1% CO₂ run agrees with results from a majority of the climate models used in the Houghton et al. (2001) report.

Our final conclusion is that the maximum northward heat transport in the North Atlantic at about 22°N is set by the maximum meridional overturning. This agrees with previous work, such as Böning et al. (1996) and Wood et al. (1999). The maximum overturning decreases during the 1% CO₂ run, but in the doubled CO₂ run, it is recovering back toward the values found in the control run. However, in the CCSM2, variations in the vertical flow across 1-km depth between 60° and 65°N do not appear to affect the northward heat transport poleward of 62°N.

Acknowledgments. We would like to thank all of the scientists and software engineers who have contributed to the development of the Community Climate System Model, version 2.

REFERENCES

- Barnett, T. P., D. W. Pierce, and R. Schnur, 2001: Detection of anthropogenic climate change in the world's oceans. *Science*, **292**, 270–274.
- Böning, C. W., F. O. Bryan, W. R. Holland, and R. Doscher, 1996: Deep-water formation and meridional overturning in a high-resolution model of the North Atlantic. *J. Phys. Oceanogr.*, **26**, 1142–1164.
- Bryan, F. O., 1998: Climate drift in a multicentury integration of the NCAR Climate System Model. *J. Climate*, **11**, 1455–1471.
- Danabasoglu, G., J. C. McWilliams, and P. R. Gent, 1994: The role of mesoscale tracer transports in the global ocean circulation. *Science*, **264**, 1123–1126.
- Dukowicz, J. K., and R. D. Smith, 1994: Implicit free-surface formulation of the Bryan-Cox-Semtner ocean model. *J. Geophys. Res.*, **99**, 7991–8014.
- Gent, P. R., 2001: Will the North Atlantic Ocean thermohaline circulation weaken during the 21st century? *Geophys. Res. Lett.*, **28**, 1023–1026.
- , and J. C. McWilliams, 1990: Isopycnal mixing in ocean circulation models. *J. Phys. Oceanogr.*, **20**, 150–155.
- , A. P. Craig, C. M. Bitz, and J. W. Weatherly, 2002: Parameterization improvements in an eddy-permitting ocean model for climate. *J. Climate*, **15**, 1447–1459.
- Griffies, S. M., 1998: The Gent–McWilliams skew flux. *J. Phys. Oceanogr.*, **28**, 831–841.
- Hall, M. M., and H. L. Bryden, 1982: Direct estimates and mechanisms of ocean heat transport. *Deep-Sea Res.*, **29**, 339–359.
- Holland, M. M., 2003: The North Atlantic Oscillation–Arctic Oscillation in the CCSM2 and its influence on Arctic climate variability. *J. Climate*, **16**, 2767–2781.
- Houghton, J. T., Y. Ding, D. J. Griggs, M. Noguera, P. J. van der Linden, and D. Xiaosu, Eds., 2001: *Climate Change 2001: The Scientific Basis*. Cambridge University Press, 881 pp.
- Kiehl, J. T., and P. R. Gent, 2004: The Community Climate System Model, version 2. *J. Climate*, **17**, 3666–3682.
- Large, W. G., J. C. McWilliams, and S. C. Doney, 1994: Oceanic vertical mixing: A review and a model with a nonlocal boundary layer parameterization. *Rev. Geophys.*, **32**, 363–403.
- Levitus, S., T. Boyer, M. Conkright, D. Johnson, T. O'Brien, J. Antonov, C. Stephens, and R. Gelfand, 1998: *Introduction*. Vol. 1, *World Ocean Database 1998*, NOAA Atlas NESDIS 18, 346 pp.
- , J. I. Antonov, T. P. Boyer, and C. Stephens, 2000: Warming of the World Ocean. *Science*, **287**, 2225–2229.
- , —, J. Wang, T. L. Delworth, K. W. Dixon, and A. J. Broccoli, 2001: Anthropogenic warming of earth's climate system. *Science*, **292**, 267–270.
- McDougall, T. J., D. R. Jackett, D. G. Wright, and R. Feistel, 2003: Accurate and computationally efficient algorithms for potential temperature and density of seawater. *J. Atmos. Oceanic Technol.*, **20**, 730–741.
- Reichert, B. K., R. Schnur, and L. Bengtsson, 2002: Global ocean warming tied to anthropogenic forcing. *Geophys. Res. Lett.*, **29**, 1525–1528.
- Roemmich, D., and C. Wunsch, 1985: Two transatlantic sections: Meridional circulation and heat flux in the subtropical North Atlantic Ocean. *Deep-Sea Res.*, **32**, 619–664.
- Saenko, O. A., A. J. Weaver, and A. Schmittner, 2003: Atlantic deep circulation controlled by freshening in the Southern Ocean. *Geophys. Res. Lett.*, **14**, 1754–1757.
- Smagorinsky, J., 1963: General circulation experiments with the primitive equations. *Mon. Wea. Rev.*, **91**, 99–164.
- Smith, R. D., and P. R. Gent, cited 2002: Reference manual for the Parallel Ocean Program (POP): Ocean component of the Community Climate System Model (CCSM2.0 and CCSM3.0). Los Alamos National Laboratory Tech. Rep. LA-UR-02-2484. [Available online at <http://www.cesm.ucar.edu/models/ccsm2.0/pop/>]
- , and J. C. McWilliams, 2003: Anisotropic horizontal viscosity for ocean models. *Ocean Modell.*, **5**, 129–156.
- , J. K. Dukowicz, and R. C. Malone, 1992: Parallel ocean general circulation modeling. *Physica D*, **60**, 38–61.
- Steele, M., R. Morley, and W. Ermold, 2001: PHC: A global ocean hydrography with a high-quality Arctic Ocean. *J. Climate*, **14**, 2079–2087.
- Sun, S., and J. E. Hansen, 2003: Climate simulations for 1951–2050 with a coupled atmosphere–ocean model. *J. Climate*, **16**, 2807–2826.
- Thorpe, R. B., J. M. Gregory, T. C. Johns, R. A. Wood, and J. F. B. Mitchell, 2001: Mechanisms determining the Atlantic thermo-

- haline circulation response to greenhouse gas forcing in a non-flux-adjusted coupled climate model. *J. Climate*, **14**, 3102–3116.
- Trenberth, K. E., and J. M. Caron, 2001: Estimates of meridional atmosphere and ocean heat transports. *J. Climate*, **14**, 3433–3443.
- Wood, R. A., A. B. Keen, J. F. B. Mitchell, and J. M. Gregory, 1999: Changing spatial structure of the thermohaline circulation in response to atmospheric CO₂ forcing in a climate model. *Nature*, **399**, 572–575.